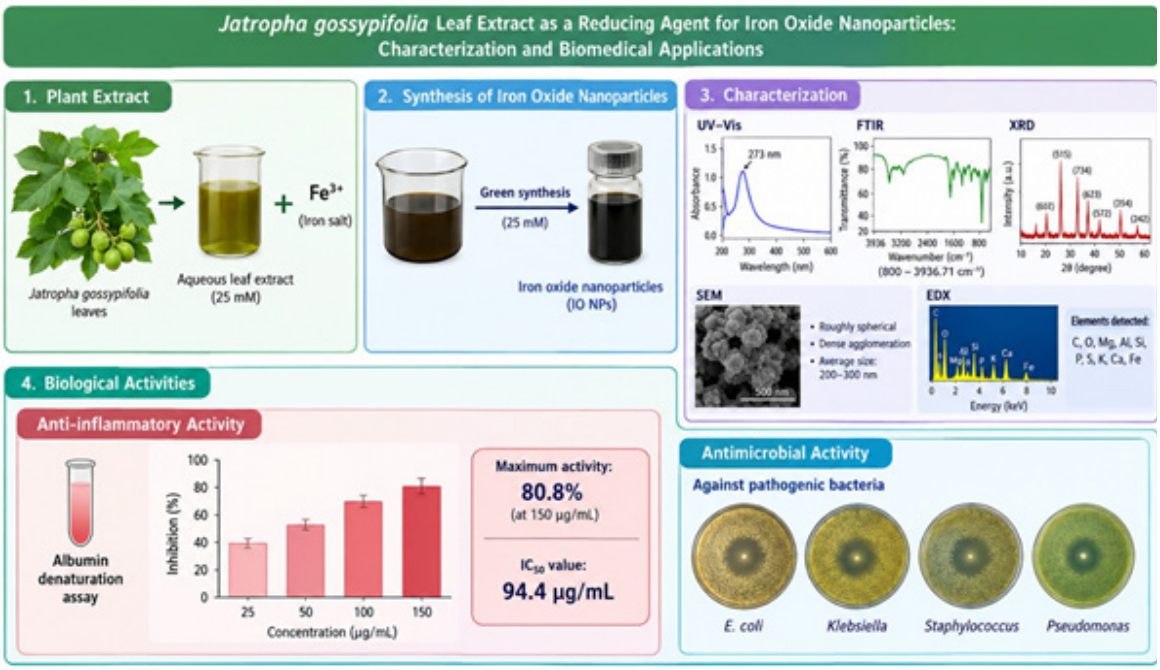
RESEARCH ARTICLE

Jatropha gossypifolia Leaf Extract as a Reducing Agent for Iron Oxide Nanoparticles: Characterization and Biomedical Applications

C.M. Archana, E. Kaarunya, P. Umamaheshwari, C. Devadharshini and G. Anbarasi

Graphical Abstract



Highlights

- Iron oxide nanoparticles were synthesized using *Jatropha gossypifolia* leaf extract.
- Nanoparticles were characterized using UV, FTIR, XRD, SEM, and EDX analyses.
- The nanoparticles exhibited 80.8% anti-inflammatory activity at 150 µg/mL.
- Antimicrobial activity was evaluated against four bacterial groups.

Ceylon Journal of Science 55 (4) 2026: 1722-1734
DOI: https://doi.org/10.4038/cjs.v55i4.9109

RESEARCH ARTICLE

Jatropha gossypifolia Leaf Extract as a Reducing Agent for Iron Oxide Nanoparticles: Characterization and Biomedical Applications

C.M. Archana[1]*, E. Kaarunya[1], P. Umamaheshwari[1], C. Devadharshini[1] and G. Anbarasi[2]

[1] *Department of Microbiology, Thiagarajar College, Madurai – 625009, Tamil Nadu, India*
[2] *Department of Biotechnology, PSGR Krishnammal College for Women, Coimbatore –641004, Tamil Nadu, India*

Received: 11.08.2025 *Accepted: 19.10.2026*

Abstract

Herbal medicines are widely used throughout the world and are considered to be safe, providing a promising avenue for the development of various therapeutic products. Iron oxide nanoparticles have attracted considerable attention because of their remarkable properties, including superparamagnetism, large surface area, and a high surface-area-to-volume ratio. They have also been investigated for various applications in therapeutic, agricultural, and environmental research. In this study, iron oxide nanoparticles were synthesised using an aqueous extract of *Jatropha gossypifolia* leaves at a concentration of 25 mM. The leaves of *J. gossypifolia* are rich in terpenoids and other phytochemicals. The synthesised iron oxide nanoparticles were characterised using UV analysis, which showed an absorption peak at 273 nm. Fourier-transform infrared (FTIR) analysis of the green-synthesised iron oxide nanoparticles revealed several absorption peaks between 800 and 3936.71 cm^{-1}. X-ray diffraction (XRD) analysis revealed diffraction peaks at 14.22° (515), 21.30° (734), 27.68° (601), 28.17° (623), 32.06° (572), 46.07° (354), and 55.27° (242). Scanning electron microscopy (SEM) revealed that the synthesised nanoparticles were roughly spherical and exhibited dense agglomeration, with an average particle size of 200–300 nm. Energy-dispersive X-ray spectroscopy (EDX) revealed the presence of C, O, Mg, Al, Si, P, S, K, Ca, and Fe in the synthesised nanoparticles. An albumin denaturation assay was performed to evaluate the anti-inflammatory activity of the nanoparticles, which was 80.8% at a concentration of 150 µg/mL, with an IC_{50} value of 94.4 µg/mL. The antimicrobial activity of the synthesised nanoparticles was evaluated against *Escherichia coli*, *Klebsiella* spp., *Staphylococcus* spp., and *Pseudomonas* spp.

Keywords: Antibacterial; Biocompatibility; *Jatropha*; Phytosynthesis; Superparamagnetism

INTRODUCTION

Herbal medicine is a cornerstone of alternative and complementary medicine, which has recently gained considerable acceptance throughout the world and is progressively making its way into established healthcare systems. Herbal medicine includes all the medicinal products that are prepared by using plants, plant parts, or plant products, with minimal or no chemical manipulation (Parveen et al., 2020). Herbal medicine is used to treat a variety of conditions, including diabetes, high blood pressure, cancer, and mental disorders. It has grown in popularity in recent years as more and more people seek a natural, holistic approach to health care.

The genus *Jatropha* belongs to the *Joannesieae* subfamily of Euphorbiaceae family, and it includes about 175 species. Linnaeus described it for the first time in 1737. Most notable species of the genus include *Jatropha gossypifolia, Jatropha curcas, Jatropha isabellei, Jatropha interrigma,* and *Jatropha macrorhiza* (Cavalcante et al., 2020*).* One of the most significant species is *Jatropha gosypifolia.* It is also known as bellyache bush or cotton-leaved physic nut, is a small shrub or tree that belongs to the Euphorbiaceae family, which grows wildly almost throughout India. The name *Jatropha* comes from the Greek word "jatros" meaning 'doctor' and "trophe" meaning 'food' (Zengin et al., 2021). It usually presents in open, sunny places (Islam et al., 2019). *J. gossypifolia* is an erect, monoecious, deciduous, soft-wooded, and perennial shrub which grows with an average height of 2.5 m but exceeds 4 m in some places. The leaves are sticky, covered with extrafloral nectaries, deeply 3-lobed and bronze when juvenile but green when mature. The flower is reddish purple in colour

**Corresponding Author's Email:drarchanamilton@gmail.com*
https://orcid.org/0009-0009-5059-2458

This article is published under the Creative Commons Attribution License (https://creativecommons.org/licenses/by/4.0/), which permits unrestricted use, distribution, and reproduction in any medium, provided the original work is properly cited.

and the flowering season is between April and August. Fruits are triocular, one seed per locule, explosively dehiscent capsules. Capsules are green in colour at maturity, which turn pale green before dehiscence and are sparsely hairy. The seeds are round, carunculate, greyish-brown, and have a lot of starchy endosperm. It is a thorny, gregarious shrub that primarily thrives in India (Saleem et al., 2016).

Nanoparticles are defined as particles ranging between 1-100nm in size. Different metallic nanoparticles are being produced using silver, iron, zinc, copper, gold, platinum, titanium, and alginate. Metal and metal oxide nanoparticles, which include iron oxide, zinc oxide, and copper oxide is most used in industries and studied for their effects on different plant parts. Iron oxide nanoparticles (IO NPs) are a class of materials that have gained significant attention in recent years due to their unique properties and potential applications in various fields such as biomedicine, electronics, and energy storage. One of the most notable properties of IO NPs is their magnetic behaviour. IO NPs exhibit superparamagnetism, which means that they can be easily magnetized and demagnetized by an external magnetic field. This property makes IO NPs attractive for use in magnetic resonance imaging (MRI) contrast agents, where they can be used to enhance the visibility of certain tissues in the body. IO NPs also have unique catalytic properties that make them attractive for use in various chemical reactions. Iron oxide nanoparticles have also been explored as a potential material for use in energy storage devices, such as lithium-ion batteries. Iron oxide nanoparticles have been shown to have a high lithium-ion storage capacity and good cycling stability. This makes them a promising material for use in lithium-ion batteries, which are widely used in portable electronics and electric vehicles. Iron oxide nanoparticles have been shown to be effective at removing pollutants such as heavy metals and organic compounds from water. This makes Iron oxide nanoparticles a promising material for use in water treatment systems (Maharjan et al., 2020).

Inflammation is a common cause of many different types of illness problems, including arthritis, cardiovascular disease, and asthma. Inflammation is a pathophysiological condition characterized by a biological response of bodily tissues to physical, chemical, and biological stimuli. Immune cells, blood vessels, and chemical mediators all participate in this process, which removes damage and initiates tissue healing. On the other hand, chronic inflammation can promote the formation of several diseases. Several anti-inflammatory medications have been created over time with the intention of lowering the inflammatory mediators' levels in the body (Frattaruolo et al., 2019). Anti-inflammatory drugs, both steroidal and non-steroidal, are currently used to treat inflammatory conditions. These drugs work by inhibiting the metabolism of arachidonic acid via the enzymes lipoxygenase and cyclooxygenase. Non-steroidal and steroidal anti-inflammatory medicines utilize anti-inflammatory chemicals known to demonstrate various adverse actions. This activity necessitates the use of isolated chemicals with lower toxicological latency. Ibuprofen, a non-steroidal anti-inflammatory drug have greater risk of heart attack and stroke and these could be fatal. Hence, look for plant-based medicines that have protective effects and have few side effects overall, essentially drawing the best anticipation for humans. Anti-inflammatory assays are performed to evaluate the ability of *J. gossypifolia* to modulate the inflammatory response. These assays are essential in determining the anti-inflammatory properties of the plant and identifying the active compounds responsible for these properties (Gabriel et al., 2020).

Multidrug-resistant (MDR) microorganisms pose a hazard to the entire world and have made it difficult to treat many infectious diseases effectively. In the past, infections had been successfully controlled by the discovery of antibiotics. Several other factors, such as ageing, transplant problems, stress, and the prevalence of immune-compromised people, contribute to antibiotics' reduced effectiveness. Several secondary metabolites found in plants are useful for treating a variety of ailments. Small-molecular-weight phytochemicals, often known as phytoalexins or phytochemicals, have less antibacterial action than conventional antibiotics (typically MW less than 500). The phenomenon of antibiotic resistance can be effectively managed through the synergistic interaction of natural substances with the currently accessible antibiotics. The term "synergism" is used when two substances combined therapeutic impact is greater than their individual effects. The interaction of an antimicrobial agent with its target inside the pathogen may be improved or made easier by the combination of natural substances, which would stop the development of resistance. This approach also lowers toxicity since lower concentrations are used. Due to the important role medicinal plants play in the process of drug discovery and development, they are widely recognized as sources of active antimicrobial metabolites (Ayaz et al., 2019). Hence, the present work aims to synthesize iron oxide nanoparticles from aqueous leaf extract of *J. gossypifolia* and screen for its in vitro anti-inflammatory and antimicrobial activities.

Materials and methods

Collection and preparation of plant extract

Leaves of *Jatropha gossypifolia* (family Euphorbiaceae) were collected and washed with water to remove dust particles adhering to their surfaces. The leaves were then dried at room temperature, ground into a fine powder, and stored in an airtight container for further use (Jeyapaul et al., 2018).

The aqueous leaf extract of *J. gossypifolia* was prepared using the Soxhlet extraction method. Approximately 5 g of dried leaf powder was weighed and extracted using 100 mL of water in a Soxhlet apparatus at 80 °C for 4 h. The finely ground sample was placed in the thimble of the Soxhlet

apparatus. The extraction solvent was heated in the bottom flask, and the resulting vapour passed through the sample thimble, condensed in the condenser, and dripped back into the thimble. When the liquid reached the siphon arm, it was transferred back into the bottom flask, and the process continued (Mahire & Patel, 2020).

Phytochemical analysis

Screening tests were performed to identify bioactive chemical constituents in the plant extract.

Flavonoids

A 2 mL aliquot of the extract was placed in a test tube and mixed with 2 mL of 2% NaOH solution. The formation of an intense yellow colour, which disappeared upon the addition of a few drops of dilute acid, indicated the presence of flavonoids (Hossain et al., 2013).

Glycosides

A 1 mL aliquot of the extract was mixed with 1 mL of concentrated H_2SO_4. The mixture was allowed to stand for 2 min. The formation of a reddish colour indicated the presence of glycosides.

Saponins

A 2 mL aliquot of the leaf extract was mixed with 3 mL of distilled water in a test tube and shaken vigorously. The formation of stable foam indicated the presence of saponins.

Tannins

A 2 mL aliquot of the extract was mixed with 2 mL of 2% $FeCl_3$ solution. The formation of a black colour indicated the presence of tannins (Auwal et al., 2014).

Terpenoids

A 2 mL aliquot of the extract was placed in a test tube, and copper acetate was added. The formation of a green colour indicated the presence of terpenoids.

Steroids

A 2 mL aliquot of the extract was mixed with 2 mL of chloroform. Concentrated H_2SO_4 was then added carefully along the side of the test tube. The formation of a red colour in the lower chloroform layer indicated the presence of steroids (Yadav & Agarwala, 2011).

Carbohydrates

A 1 mL aliquot of the extract was mixed with 2 mL of Benedict's reagent. The mixture was heated in a boiling water bath for 3–5 min. The formation of a green, yellow, orange, or red colour indicated the presence of reducing sugars at different concentrations (Shaikh & Patil, 2020).

The colour changes were interpreted as follows:

Green: 0.5%

Yellow: 1%

Orange: 1.5%

Red: 2%

Proteins

A 2 mL aliquot of the extract was mixed with 2 mL of 0.2% ninhydrin solution. The formation of a violet colour indicated the presence of amino acids and proteins.

Phenols

The leaf extract was treated with 3–4 drops of ferric chloride solution. The formation of a bluish-black colour indicated the presence of phenolic compounds (Nikam & Namdas, 2022).

Biosynthesis of iron oxide nanoparticles:

A 0.01 M $FeCl_3$ solution was prepared by dissolving 0.16 g of $FeCl_3$ in 100 mL of distilled water. Solutions of $FeCl_3$ at concentrations of 0.005 M and 0.0025 M were also prepared. For the synthesis of iron oxide nanoparticles, 10 mL of the aqueous leaf extract of *J. gossypifolia* was mixed in a 1:1 ratio with an equal volume of $FeCl_3$ solutions at concentrations of 0.001 M, 0.0005 M, and 0.00025 M. The mixtures were shaken overnight. Nanoparticle formation was assessed based on the colour change of the solutions. The appearance of a black colour indicated the formation of iron oxide nanoparticles. Of the concentrations tested, the lowest concentration, 0.00025 M, was selected. Following synthesis, the sample was centrifuged, and the resulting pellet was dried. The dried nanoparticles were stored in an airtight container for further investigation (Kanagasubbulakshmi & Kadirvelu, 2017).

Characterization of nanoparticles

Ultraviolet – visible (UV-VIS) spectrophotometric analysis

UV–Vis spectrophotometry was used as a preliminary method to assess nanoparticle synthesis. Following exposure of the precursor solution to the plant extract, the resulting sample was analysed using UV–Vis spectrophotometry. The instrument measured the intensity of light transmitted through the sample at different wavelengths.

FT-IR (Fourier- transform spectrometer) analysis

FTIR analysis was performed to investigate the functional groups associated with the plant extract and the synthesised

iron oxide nanoparticles. The particles were washed thoroughly, collected, and dried at room temperature. The FTIR spectra were recorded over the range of 400–4500 cm^{-1} (Devi et al., 2019).

XRD (X-Ray Diffraction) analysis

The crystallinity of the synthesised nanoparticles was investigated using an X-ray diffractometer. X-ray diffraction patterns of the powdered nanoparticle samples were recorded over a 2θ range of 10–80° (Nadeem et al., 2022).

SEM (scanning electron microscopy) analysis

The morphology of the synthesised iron oxide nanoparticles was examined using scanning electron microscopy (SEM). The dried nanoparticles were mounted on double-sided adhesive tape and coated with platinum before imaging (Zakariya et al., 2022).

EDX (energy-dispersive X-ray spectroscopy) analysis

The elemental composition of the synthesised iron oxide nanoparticles was analysed using energy-dispersive X-ray spectroscopy (EDX) coupled with SEM (Vishalatchi et al., 2022).

Anti-inflammatory activity of synthesized iron oxide nanoparticles from *Jatropha gossypifolia* (inhibition of protein denaturation assay)

The anti-inflammatory activity of the synthesised iron oxide nanoparticles was evaluated using an albumin denaturation inhibition assay. The reaction mixture consisted of different concentrations of the test sample and a 1% aqueous solution of bovine serum albumin. The pH of the reaction mixture was adjusted by adding a small quantity of 1 N HCl. The samples were incubated at 37 °C for 20 min and then heated at 51 °C for 20 min. After cooling, the turbidity was measured at 660 nm using a UV–Vis spectrophotometer.

The following formula was used to calculate the Percentage inhibition of protein denaturation:

$$\text{Percentage inhibition} = \frac{\text{Absorbance of control} - \text{Absorbance of sample}}{\text{Absorbance of control}} \times 100$$

The IC_{50} value was defined as the concentration of the sample to inhibit 50% of protein denaturation under assay condition (Dharmadeva et al., 2018).

Antimicrobial activity of synthesized iron oxide nanoparticles of *Jatropha gossypifolia*

The antibacterial activity of the iron oxide nanoparticles synthesised using *J. gossypifolia* was evaluated against Gram-positive and Gram-negative bacteria using the well-diffusion method. The bacterial species tested were *Escherichia coli*, *Klebsiella spp*., *Staphylococcus aureus*, and *Pseudomonas spp*. The bacterial strains were spread over the surfaces of Petri dishes containing autoclaved Mueller–Hinton agar. Wells were made in the agar, and the synthesised iron oxide nanoparticle suspensions at various concentrations were added to the wells. The plates were incubated at 37 °C for 24 h, after which the zones of inhibition were measured (Sandhya & Kalaiselvam, 2020).

RESULTS AND DISCUSSION

Preparation of plant extracts

The leaves of *Jatropha gossypifolia* have been collected aseptically in K. Meenachipuram, Aruppukottai Taluk, Virudhunagar district. The leaves were washed to remove the dirt on the surface of the leaves and then shade dried. The dried leaves were grinded and kept for further use. Soxhlet extraction method is used to obtain the aqueous leaf extract of *Jatropha gossypifolia*. 5 g of powdered sample was extracted using 100 ml of water in Soxhlet apparatus at 80°C for 4 h. Finally, 90 ml of aqueous leaf extract was obtained (Figure 1).

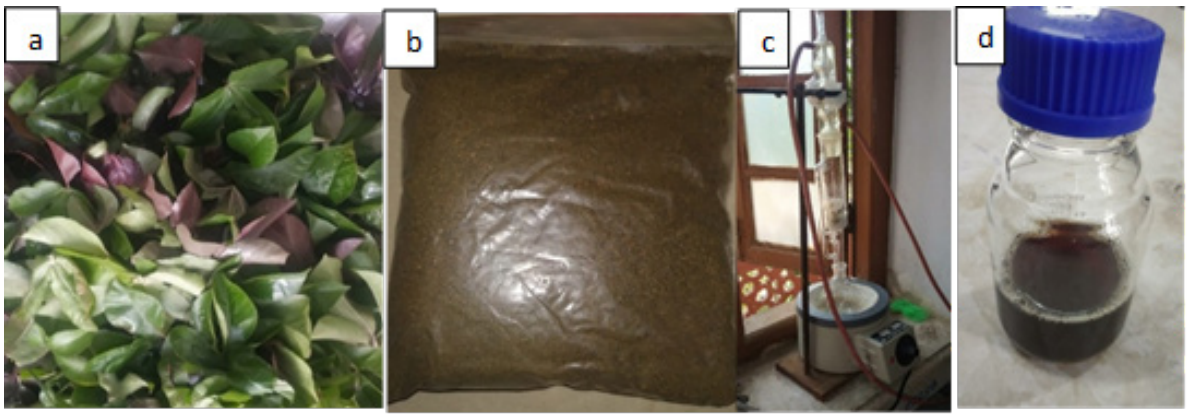


Figure 1: Aqueous extraction of *Jatropha gossypifolia* leaves: (a) leaves; (b) powdered leaves; (c) Soxhlet extraction apparatus; (d) aqueous leaf extract

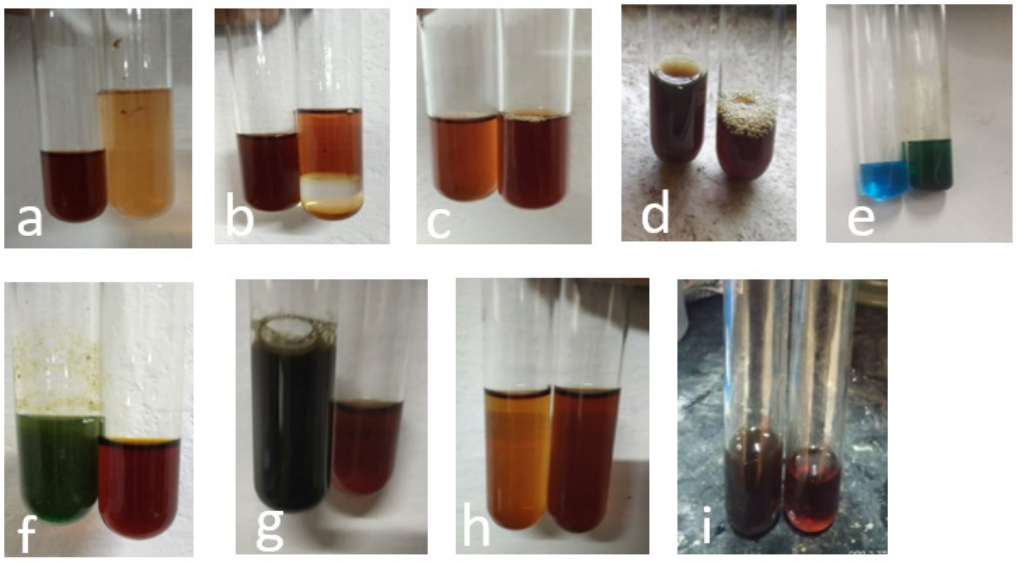


Figure 2: Qualitative phytochemical analysis of the aqueous leaf extract of *Jatropha gossypifolia*: (a) carbohydrates; (b) flavonoids; (c) glycosides; (d) phenols; (e) proteins; (f) saponins; (g) steroids; (h) tannins; and (i) terpenoids

Qualitative phytochemical screening of *Jatropha gossypifolia* leaf extract

Preliminary phytochemical analysis was carried out to determine the presence or absence of selected phytochemical constituents according to standard methods. Tannins, saponins, flavonoids, alkaloids, steroids, carbohydrates, terpenoids, and cardiac glycosides were found in the aqueous leaf extract of *Jatropha gossypifolia* (Figure 2). The results of phytochemical analysis are presented in Table 1. The presence of flavonoids accounts for its anti-inflammatory action in *J. gossypifolia*. The presence of phenols, tannins, and flavonoids accounts for the antioxidant activity (Dias et al., 2019). Carbohydrates itself does not have any therapeutic effect, but provides a better therapeutic effect with the combination of other active principles in each plant. Saponins have also been reported to have hypoglycemic and anti-diabetic effects (Auwal et al., 2014).

The phytochemical analysis of the aqueous leaf extract of *Jatropha gossypifolia* revealed the presence of flavonoids, glycosides, saponins, terpenoids, steroids, carbohydrates, tannins, and phenols, while proteins were absent.

Synthesis and characterization of iron oxide nanoparticles

Synthesis of iron oxide nanoparticles

The biosynthesis of FeO NPs from aqueous leaf extract of *Jatropha gossypifolia* was extensively studied. The preliminary test to observe the colour change confirmed the formation of FeO NPs. Three different concentrations 25mM, 50mM, 100mM of $FeCl_3$ solutions were used. The appearance of brownish-black colour within 24 hours indicates the formation of Iron oxide nanoparticles in the solution. Compared to the 25mM, 50mM, 100mM were darker. Among the three different concentrations, the lowest concentration (25mM) was chosen for further examination. The plant extract contains active constituents that played a double role as a reducing and capping agent for the green synthesis of nanoparticles.

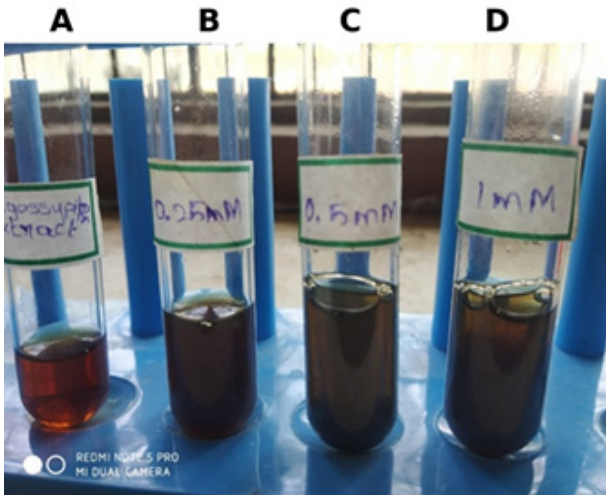


Figure 3: Screening of *Jatropha gossypifolia* leaf extract for IONP synthesis: (A) leaf extract alone; (B–D) leaf extract mixed with $FeCl_3$ at concentrations of 0.25, 0.5 and 1 mM, respectively. Darker colour indicates nanoparticle formation

In the green synthesis of iron oxide nanoparticles using *Moringa oleifera* leaf extract, UV-Vis spectroscopy confirmed the noticeable color change to dark brown, which indicates the presence of iron oxide nanoparticles (Jadhav et al., 2022). The change in colour and thickness of the colour was taken as primary evidence for the formation of Iron oxide nanoparticles (Figure 3). The formation of light brown and black colours indicates the presence of iron oxide nanoparticles synthesized using *Eucalyptus globulus* Extract (Zaveleta et al., 2022).

UV-Vis spectrophotometry of synthesized iron oxide nanoparticles

Characterization by UV-vis spectrometry was considered as a preliminary analysis to show the synthesis of nanoparticles. The maximum absorbance of the Iron oxide nanoparticles synthesized using the leaf extract of *Jatropha gossypifolia* was observed at 273nm. This indicates the formation of Iron oxide nanoparticles. The graphical representation of UV-vis spectroscopy of IO NPs was given in Figure 4.

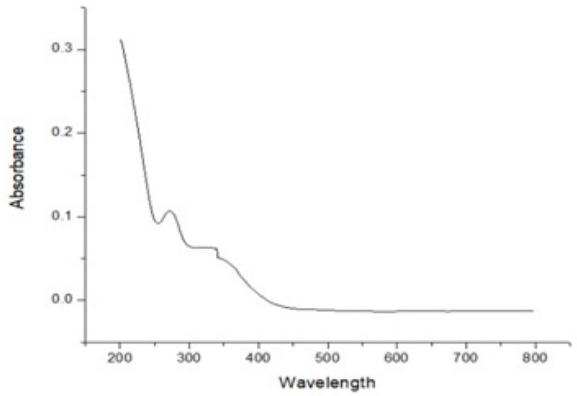


Figure 4: UV–visible absorption spectrum of iron oxide nanoparticles (IONPs) synthesized using *Jatropha gossypifolia* leaf extract.

The characteristic absorption peak formation of iron oxide nanoparticles synthesized using *Pometia pinnata* was observed at 272-297 nm. In the synthesis of IO NPs using *Aesculus hippocastanum*, UV-Vis spectroscopy was observed in the wavelength range of 250-300nm (Weerasinghe et al., 2023). The presence of a strong peak at around 242 nm was attributed to the formation of iron oxide nanoparticles synthesized using neem leaf extract (Zambri et al., 2019).

FT-IR analysis of synthesized iron oxide nanoparticles

The FTIR analysis has been used to identify the functional groups present in the synthesized iron oxide nanoparticles. The FTIR analysis of green synthesized IO NPs revealed many absorption peaks between 800 cm^{-1} and 3936.71 cm^{-1}. The peaks were obtained at 3936.71, 3886.56, 3873.06, 3853.77, 3840.27, 3784.34, 3776.62, 3768.91, 3682.11, 3660.89, 3066.82, 2926.01, 2308.79, 1743.65, 1512.19, 1039.63, 802.39 cm^{-1}. The graphical representation of the FTIR analysis of IO NPs was represented (Figure 5). The strong instance peak was identified at 3936.71 cm^{-1} which is assigned to the O-H bond stretch of hydroxyl group. The peaks at 3886.56, 3873.06, 3853.77, 3840.27, 3784.34, 3776.62, 3768.91, 3682.11, 3660.89, 3066.82 cm^{-1} were assigned to the stretching vibration of O-H bond. The peak at 2926.01 cm^{-1} was assigned to the stretching vibration of C-H bond. The peak at 2308.79 cm^{-1} was assigned to the CO_2 bending vibration. The peak at 1743.65 cm^{-1} was assigned to the stretching vibration of C=O bond. The peak at 1512.19 cm^{-1} was assigned to the stretching vibration of O-H bond. The peak at 1039.63 cm^{-1} was assigned to the symmetric stretching mode of FeO bond. The peak at 802.39 cm^{-1} was assigned to FeO bending vibration. The FTIR spectrum confirmed the presence of functional groups associated with the biomolecules involved in the synthesis and stabilization of IO NPs (Table 2).

FTIR spectrum of IO NPs synthesized using *Sesbania grandiflora* shows the following peaks (Figure 5). The peaks at 1700 cm^{-1} and 1850 cm^{-1} exhibited the C=O stretching vibrations, and the strong peak at 1388 cm^{-1} indicated the aromatic amine (C-N) stretching, and the medium peak at 915 cm^{-1} was assigned to carboxylic acid (O-H) bending vibrations. The peak was found at a frequency of 669 cm^{-1} due to Fe-O bond vibration. The peaks at 1649 cm^{-1} and 1039 cm^{-1} corresponded to the >C=O asymmetric stretching and COO− symmetric stretching (Rajendran and Sengodan, 2017). The –OH groups are well-reported chemical bonds found in NPs, as they are responsible for oxidation, while carbonyl and carboxylate groups are involved in nanoparticle stabilization; further, the peak at 568 cm^{-1} also confirms the FeO NPs formation (Ndou *et al.,*2023). The FTIR spectra of the synthesized iron oxide nanoparticles were recorded between 3500 cm^{-1} and 400 cm^{-1}. The O−H stretching vibrations interacting through H bonds were observed at around 3430 cm^{-1}, 2927 cm^{-1}. The absorption bands present at about 585 cm^{-1} and 410 cm^{-1} was due to the stretching vibrations of metal oxide (Parhizkar et al.,2019).

XRD analysis of synthesized iron oxide nanoparticles

The XRD analysis was used to obtain information about the crystalline structure, nature of the phase, lattice parameters, and grain size. The characteristic diffraction peaks of the iron oxide nanoparticles were observed at 14.22° (515), 21.30° (734), 27.68° (601), 28.17° (623), 32.06° (572), 46.07° (354), 55.27° (242). The above peaks at corresponding planes confirms the presence of iron oxide nanoparticles. The graphical representation of XRD analysis was given in figure 6.

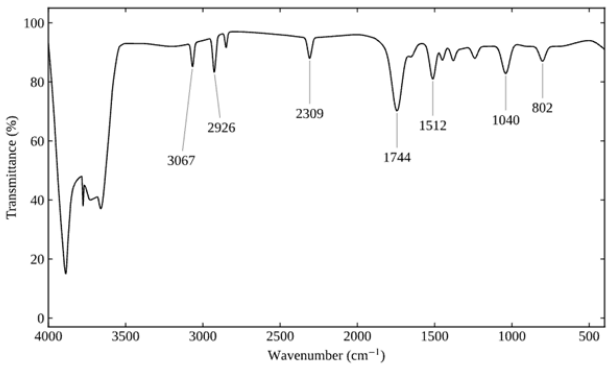


Figure 5: FTIR spectrum of iron oxide nanoparticles (IONPs) synthesized using *Jatropha gossypifolia* leaf extract

Table 1: FTIR peak values of iron oxide nanoparticles (IONPs) synthesized using Jatropha gossypifolia leaf extract

Wavenumber (cm^{-1})	Functional Group	Assignment	Role in Synthesis
3066.82	Aromatic C–H	Stretching vibration	Plant biomolecules
2926.01	Aliphatic C–H	Stretching vibration	Organic capping agents
1743.65	C=O	Carbonyl stretching	Polyphenols/proteins
1512.19	C=C / N–H	Aromatic/amide vibration	Biomolecular interaction
1039.63	C–O	Alcohol/Ether stretching	Stabilization of nanoparticles
802.39	Fe–O	Metal–oxygen vibration	Confirms iron oxide formation

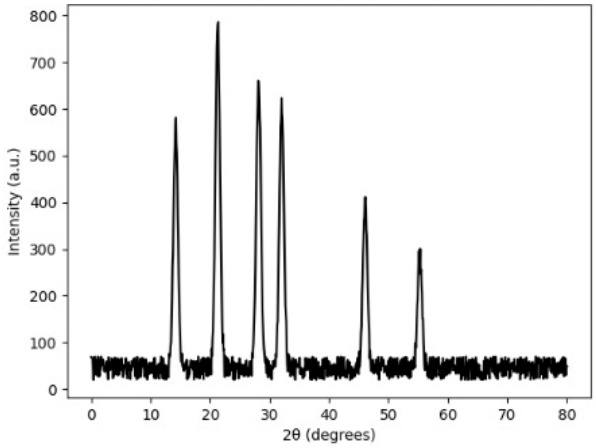


Figure 6: XRD pattern of iron oxide nanoparticles (IONPs) synthesized using *J. gossypifolia* leaf extract. Sharp peaks at 2θ ≈ 14.0°, 21.3°, 28.0°, 31.9°, 46.0° and 55.1° indicate the crystalline nature of the nanoparticles

The XRD analysis of iron oxide nanoparticles synthesized using *Oryza sativa* shows peaks at 30.29°, 35.67°, 43.34°, 53.99°, 57.21°, and 62.93° corresponding to the crystal planes of 220, 311, 400, 422, 511, and 440 were observed which confirms the presence of iron oxide nanoparticles (Durgude et al*.,* 2022). The XRD pattern of IO nanoparticles prepared using papaya leaves have peak values for 2θ = 32.06, 45.76, 56.0 and 75.57 and the planes were (211), (222), (110) and (202) (Vishalatchi, et al*.,* 2022).

SEM analysis of synthesized iron oxide nanoparticles

SEM analysis was carried out to find the surface morphology and size range of iron oxide nanoparticles. The images of IO NPs obtained under the SEM were given in figure 7. It shows that the synthesized IO NPs were roughly spherical and there was a presence of dense agglomeration. The average size of the synthesized iron oxide nanoparticles was 200-300.

Iron oxide nanoparticles were synthesized using *Nephrolepis exaltata* and their SEM analysis shows the roughly spherical and partially dispersed shape of the synthesized IO NPs. The aggregation of the IO NPs was caused by the interaction of the magnetic nanoparticles. The extremely conglomerate form of nanoparticles served as an indicator of the formation of nanoparticles with agglomeration. SEM images revealed (Figure 7) the aggregation of IO NPs, which might also be a result of the solvent being removed and evaporated during sample preparation. Electrostatic forces cause the aggregation of IO NPs when the solvent is removed (Nadeem et al.,2022). The SEM analysis of iron oxide nanoparticles synthesized using hydrothermal method shows were roughly spherical and dense agglomeration has been taken place.

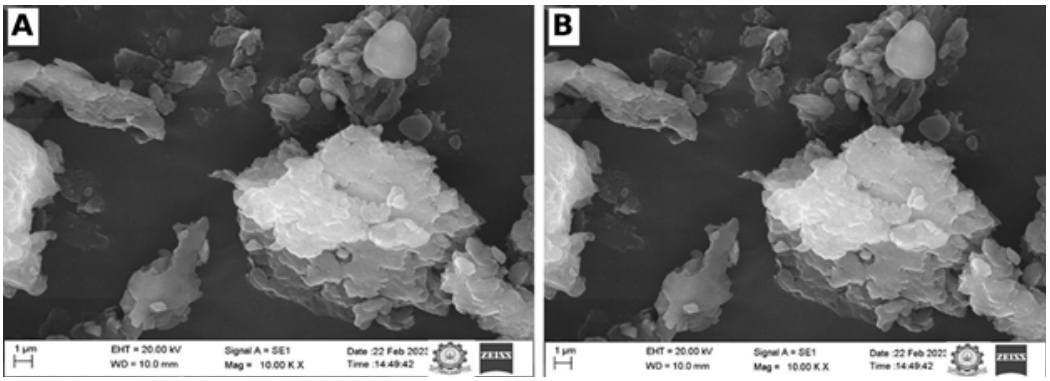
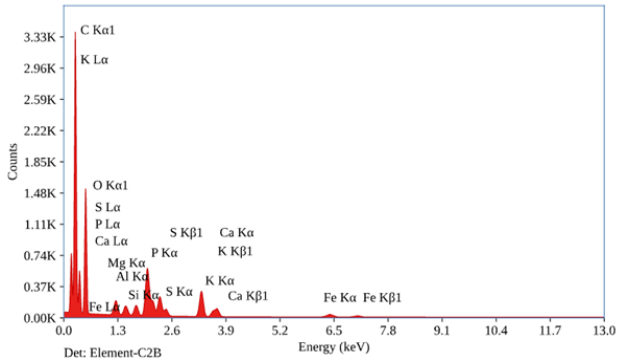


Figure 7. Scanning electron microscopy (SEM) images of iron oxide nanoparticles (IONPs) synthesized using *Jatropha gossypifolia* leaf extract. (A, B) Micrographs recorded at 10,000× magnification (scale bar = 1 µm) using a secondary electron (SE1) detector at an accelerating voltage of 20 kV and a working distance of 10.0 mm. The images show irregular, plate-like particles stacked and aggregated into larger clusters

EDX analysis of synthesized iron oxide nanoparticles

The elemental composition of the IO NPs was confirmed by the energy dispersive X-ray spectroscopy (EDS) analysis. The graphical representation of EDX analysis of the synthesized IO NPs was given in figure 8. The EDX spectra showed the presence of C, O, Mg, Al, Si, P, S, K, Ca, Fe in the IO NPs synthesized using *Jatropha gossypifolia.*

The EDX spectra of Iron oxide nanoparticles synthesized using *Sorghum bicolor* (Figure 8) showed the presence of Fe, O, Mg, Si, P, K which may be due to their presence in plant extract (Ndou et al.,2023). The EDX analysis of Iron oxide nanoparticles synthesized using fenugreek seed extract showed the presence of Fe, O, Si, Al, Mn, P, Ca (Deshmukh et al.,2019).



Smart Quant Results

Element	Weight %	Atomic %	Error %	Kratio
C K	53.9	63.8	7.9	0.2176
O K	35.4	31.4	10.8	0.0581
Mg K	1.7	1.0	8.8	0.0088
Al K	0.6	0.3	14.7	0.0035
Si K	0.6	0.3	13.6	0.0043
P K	3.7	1.7	3.7	0.0286
S K	1.0	0.4	13.2	0.0078
K K	2.1	0.8	8.9	0.0177
Ca K	0.7	0.2	18.2	0.0061
Fe K	0.6	0.1	24.4	0.0049

Figure 8: EDX of iron oxide nanoparticles (IONPs) synthesized using *Jatropha gossypifolia* leaf extract

Anti-inflammatory activity of synthesized iron oxide nanoparticles from aqueous leaf extract of *Jatropha gossypifolia*

The anti-inflammatory analysis was done to determine the anti-inflammatory activity of iron oxide nanoparticles synthesized using *J. gossypifolia* (Table 3). The rate of inhibition of protein denaturation was 10.6%, 2.52%, 39.3%, 53.7%, 80.8% at 25 µg/ml, 50 µg/ml, 75 µg/ml, 100 µg/ml, 150 µg/ml respectively. The rate of inhibition of albumin denaturation was at maximum of 80.8% in 150µg/mL concentration. The IC_{50} value was 94.4µg/ml. The graphical representation of protein denaturation by synthesized iron oxide nanoparticles was represented (figure: 9). Protein denaturation has been well correlated with the occurrence of the inflammatory response. The ability of the material to inhibit the denaturation of proteins signifies the potential for anti-inflammatory activity (Aafreen et al.,2019). Proteins typically lose their biological function as a result of protein denaturation, which involves the destruction of the secondary and tertiary structures of proteins. Heat, electrolytes, or alcohols can all cause protein denaturation, which results in changes to the solubility of albumins and globulins. The correlation between protein denaturation and inflammation may be established, and an inhibition of protein denaturation following the addition of a chemical substance can be viewed as an anti-inflammatory action (Antonoglou et al., 2019).

Table 2: Anti-inflammatory activity of *Jatropha gossypifolia* assessed by the inhibition of protein denaturation assay

S.no	Concentration of the sample (µg/ml)	% of protein denaturation	IC_{50} Value (µg/ml)
1	25	10.6	94.4
2	50	25.2	
3	75	39.3	
4	100	53.7	
5	150	80.8	

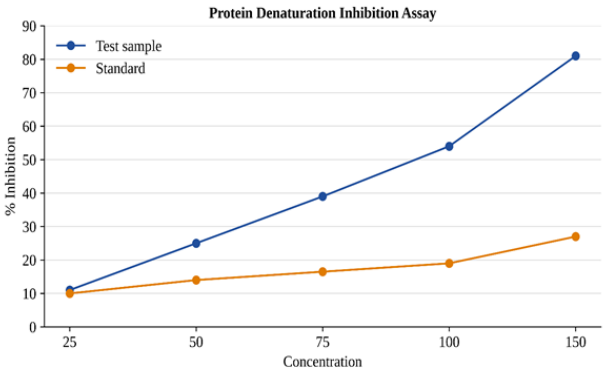


Figure 9. Protein denaturation inhibition by IONPs synthesized using *J. gossypifolia* leaf extract compared with a standard drug. Inhibition increased with concentration, reaching about 81% for the IONPs versus about 27% for the standard at 150

The anti-inflammatory activity of $CrFe_2O_4$ NPs synthesized using *Boswellia carteri* resin at concentrations of 25 and 100 µg/ml reduce expression of iNOS significantly with a percentage of 53.7% and 62.3%, respectively. A concentration of 100 µg/ml of $CrFe_2O_4$ NPs induced the IL-10 expression, anti-inflammatory gene, with a percentage

of 55.1% (Imraish et al., 2021). The percentage inhibition of protein denaturation by *Barringtonia racemosa* pericarp extract was 43.33±0.002 in 100µg/mL concentration (Osman, et al*.,* 2016). The anti-inflammatory activity of iron oxide nanoparticles synthesized using *Juglans regia* peel extract was 75.8% at 400µg/ml concentration (Abdulalsalam et al., 2017).

Antimicrobial activity of synthesized iron oxide nanoparticles from aqueous leaf extract of *Jatropha gossypifolia*

The antibacterial activities of IO NPs synthesized using *Jatropha gossypifolia* leaf extract was investigated against some pathogenic microorganisms using agar well diffusion method (Figure 10). The antimicrobial activity of the synthesized iron oxide nanoparticles against *E. coli, Klebsiella, Staphylococcus and Pseudomonas* was performed. The zone of inhibition of the each of the samples against these pathogens were noted. The pictorial representation was given in figure 10. The zone of inhibition against each pathogen was tabulated (Table 4). The zone of inhibition of the synthesized iron oxide nanoparticles against *Klebsiella pneumoniae* was 16 mm, 17 mm, 20 mm at 60 µl, 80 µl, 100 µl respectively. The zone of inhibition of the synthesized iron oxide nanoparticles against *E. coli* was 16 mm, 18 mm, 20 mm at 60 µl, 80 µl, 100 µl respectively. The zone of inhibition of the synthesized iron oxide nanoparticles against *S. aureus* was 18 mm, 20 mm, 21 mm at 60 µl, 80 µl, 100 µl respectively. The zone of inhibition of the synthesized iron oxide nanoparticles against *P. aeruginosa* was 16 mm, 19 mm, 21 mm at 60 µl, 80 µl, 100 µl respectively. The zone of inhibition was found to be highest against *Staphylococcus* and *Pseudomonas* (21 mm) and lowest against *E. coli* and *Klebsiella* (16 mm).

Due to a number of interactions, iron oxide nanoparticles have the potential to be toxic to microbes. These interactions include membrane depolarization, which compromises cell integrity, the production of reactive oxygen species (ROS), which causes DNA damage and lipid peroxidation, and the release of metal ions, which affect cellular homeostasis and protein coordination. Iron oxide nanoparticles have antimicrobial activity against certain pathogens which include *E. coli, Staphylococcus aureus, Pseudomonas aeruginosa, Klebsiella pneumoniae, Bacillus subtilis* and *Aspergillus niger* (Arias et al., 2018). The iron oxide nanoparticles synthesized by hydrothermal method have shown significant antimicrobial activity against *E. coli, Pseudomonas aeruginosa, Staphylococcus aureus* with zone of inhibition: 21mm, 19mm, 21mm respectively (Alangari et al., 2022).

Table 3: Antibacterial activity of iron oxide nanoparticles (IONPs) synthesized using *Jatropha gossypifolia* leaf extract against pathogenic bacteria, measured as zone of inhibition (mm) by the agar well diffusion method

Pathogen	60 µL	80 µL	90 µL
Escherichia coli	16	18	20
Staphylococcus aureus	18	20	21
Klebsiella pneumoniae	16	17	20
Pseudomonas aeruginosa	16	19	21

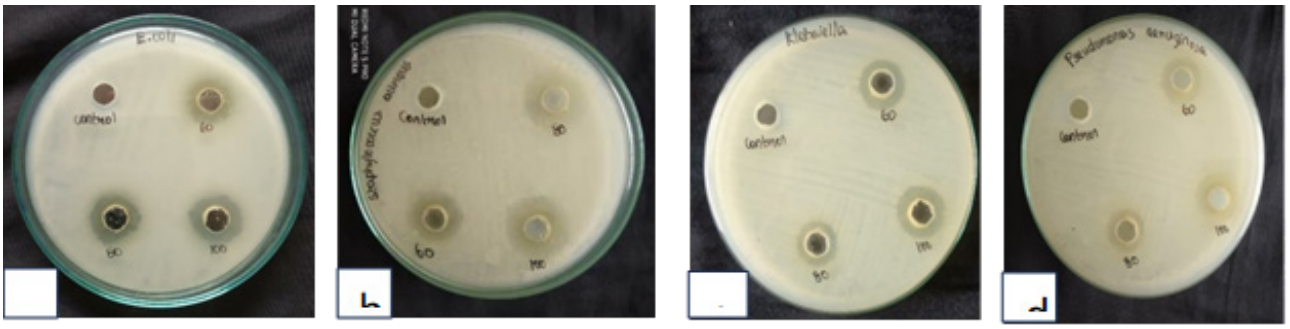


Figure 10: Antimicrobial activity of IONPs synthesized using *Jatropha gossypifolia* leaf extract against (a) *E. coli*, (b) *S. aureus*, (c) *K. pneumoniae*, and (d) *P. aeruginosa* at 60, 80, and 90 µg/mL

CONCLUSION

Iron oxide nanoparticles were successfully synthesized using an aqueous leaf extract of Jatropha gossypifolia through green synthesis. This method is cost-effective and sustainable. The active constituents of the J. gossypifolia leaf extract act as reducing and stabilizing agents during nanoparticle synthesis. The synthesized nanoparticles were characterized using UV–Vis spectroscopy, X-ray diffraction (XRD), Fourier-transform infrared spectroscopy (FTIR), scanning electron microscopy (SEM), and energy-dispersive X-ray spectroscopy (EDX). The FeO nanoparticles exhibited significant anti-inflammatory activity and moderate antibacterial activity against selected Gram-positive and Gram-negative bacteria. These findings suggest their potential for further investigation as anti-inflammatory agents. However, further studies are needed to determine the appropriate dosages, reaction conditions, and safety profiles before their potential therapeutic applications can be established.

ACKNOWLEDGEMENT

The authors thank the Department of Microbiology, Thiagarajar College, Madurai, India, for providing the facilities and support necessary to conduct this study.

FUNDING INFORMATION

This research received no external funding.

AUTHOR CONTRIBUTION

Methodology, writing—review and editing, and final draft preparation: **C.M.A.;** writing—review and editing: **E.K.;** investigation and software analysis: **P.U.;** formal analysis, writing—original draft preparation, and review: **C.D.**; methodology, investigation, and software analysis**: G.A.**

DATA AVAILABILITY STATEMENT

The dataset generated during the current study is not publicly available, but is available from the corresponding author on reasonable request.

DECLARATION OF GENERATIVE AI AND AI-ASSISTED TECHNOLOGIES IN THE MANUSCRIPT PREPARATION PROCESS

During the preparation of this work, the authors used ChatGPT (OpenAI) to improve language and readability and Claude (Anthropic) to improve the formatting of figures and tables and to refine the wording of table captions. After using these tools, the authors reviewed and edited the content as needed and take full responsibility for the content of the publication.

REFERENCES

Alangari, A., Alqahtani, M. S., Mateen, A., Kalam, M. A., Alshememry, A., Ali, R., Kazi, M., AlGhamdi, K. M., & Syed, R. (2022). Retracted: Iron oxide nanoparticles: Preparation, characterization, and assessment of antimicrobial and anticancer activity. *Adsorption Science & Technology*, **2022**, Article 1562051. https://doi.org/10.1155/2022/1562051

Andrade-Zavaleta, K., Chacon-Laiza, Y., Asmat-Campos, D., & Raquel-Checca, N. (2022). Green synthesis of superparamagnetic iron oxide nanoparticles with *Eucalyptus globulus* extract and their application in the removal of heavy metals from agricultural soil. *Molecules*, **27**(4), Article 1367. https://doi.org/10.3390/molecules27041367

Antonoglou, O., Lafazanis, K., Mourdikoudis, S., Vourlias, G., Lialiaris, T., Pantazaki, A., & Dendrinou-Samara, C. (2019). Biological relevance of $CuFeO_2$ nanoparticles: Antibacterial and anti-inflammatory activity, genotoxicity, DNA and protein interactions. *Materials Science and Engineering: C*, **99**, 264–274.

Arias, L. S., Pessan, J. P., Vieira, A. P. M., Lima, T. M. T. D., Delbem, A. C. B., & Monteiro, D. R. (2018). Iron oxide nanoparticles for biomedical applications: A perspective on synthesis, drugs, antimicrobial activity, and toxicity. *Antibiotics*, **7**(2), Article 46.

Auwal, M. S., Saka, S., Mairiga, I. A., Sanda, K. A., Shuaibu, A., & Ibrahim, A. (2014). Preliminary phytochemical and elemental analysis of aqueous and fractionated pod extracts of *Acacia nilotica* (thorn mimosa). *Veterinary Research Forum*, **5**(2), 95–100.

Ayaz, M., Ullah, F., Sadiq, A., Ullah, F., Ovais, M., Ahmed, J., & Devkota, H. P. (2019). Synergistic interactions of phytochemicals with antimicrobial agents: Potential strategy to counteract drug resistance. *Chemico-Biological Interactions*, **308**, 294–303.

Bandyopadhyay, S., Ali, Z., Larsen, A. Å., & Ashar, A. B. (2025). Iron oxide nanoparticles: Surface chemistry and electrostatic stability influence silanization. *Colloids and Surfaces A: Physicochemical and Engineering Aspects*, **709**, Article 136123.

Cavalcante, N. B., da Conceição Santos, A. D., & da Silva Almeida, J. R. G. (2020). The genus *Jatropha* (Euphorbiaceae): A review on secondary chemical metabolites and biological aspects. *Chemico-Biological Interactions*, **318**, Article 108976.

Deshmukh, A. R., Gupta, A., & Kim, B. S. (2019). Ultrasound assisted green synthesis of silver and iron oxide nanoparticles using fenugreek seed extract and their enhanced antibacterial and antioxidant activities. *BioMed Research International*, **2019**, Article 1714358.

Devi, H. S., Boda, M. A., Shah, M. A., Parveen, S., & Wani, A. H. (2019). Green synthesis of iron oxide nanoparticles using *Platanus orientalis* leaf extract for antifungal activity. *Green Processing and Synthesis*, **8**(1), 38–45.

Dharmadeva, S., Galgamuwa, L. S., Prasadinie, C., & Kumarasinghe, N. (2018). In vitro anti-inflammatory activity of *Ficus racemosa* L. bark using albumin

denaturation method. *Ayu*, **39**(4), 239.

Dias, W. L. F., do Vale Junior, E. P., de Oliveira, M. D. D. A., Barbosa, Y. L. P., do Nascimento Silva, J., da Costa Júnior, J. S., [remaining authors to be verified], & Martins, F. A. (2019). Cytogenotoxic effect, phytochemical screening and antioxidant potential of *Jatropha mollissima* (Pohl) Baill leaves. *South African Journal of Botany*, **123**, 30–35.

Durgude, S. A., Ram, S., Kumar, R., Singh, S. V., Singh, V., Durgude, A. G., [remaining authors to be verified], & Hossain, A. (2022). Synthesis of mesoporous silica and graphene-based FeO and ZnO nanocomposites for nutritional biofortification and sustained the productivity of rice (*Oryza sativa* L.). *Journal of Nanomaterials*, **2022**, Article 5120307.

Evans, W. C. (2009). *Trease and Evans' pharmacognosy*. Elsevier Health Sciences.

Frattaruolo, L., Carullo, G., Brindisi, M., Mazzotta, S., Bellissimo, L., Rago, V., [remaining authors to be verified], & Cappello, A. R. (2019). Antioxidant and anti-inflammatory activities of flavanones from *Glycyrrhiza glabra* L. (licorice) leaf phytocomplexes: Identification of licoflavanone as a modulator of NF-κB/MAPK pathway. *Antioxidants*, **8**(6), Article 186.

Gabriel, B. O., Oshomoh, E. O., & Kevin, O. I. (2020). Anti-inflammatory and anti-nociceptive properties of aqueous leaves extract of *Ipomoea batatas* (Lam.) on experimental animals. *NIPES Journal of Science and Technology Research*, **2**(1).

Gurushankar, K., Chinnaiah, K., Kannan, K., Gohulkumar, M., & Periyasamy, P. (2021). Synthesis and characterization of FeO nanoparticles by hydrothermal method. *Rasayan Journal of Chemistry*, **14**(3), 1985–1989.

Harborne, A. J. (1998). *Phytochemical methods: A guide to modern techniques of plant analysis*. Springer Science & Business Media.

Hossain, M. A., Al-Raqmi, K. A. S., Al-Mijizy, Z. H., Weli, A. M., & Al-Riyami, Q. (2013). Study of total phenol, flavonoids contents and phytochemical screening of various leaves crude extracts of locally grown *Thymus vulgaris*. *Asian Pacific Journal of Tropical Biomedicine*, **3**(9), 705–710.

Imraish, A., Abu Thiab, T., Al-Awaida, W., Al-Ameer, H. J., Bustanji, Y., Hammad, H., [remaining authors to be verified], & Al-Hunaiti, A. (2021). In vitro anti-inflammatory and antioxidant activities of $ZnFe_2O_4$ and $CrFe_2O_4$ nanoparticles synthesized using *Boswellia carteri* resin. *Journal of Food Biochemistry*, **45**(6), Article e13730.

Islam, M. S., Ara, H., Ahmad, K. I., & Uddin, M. M. (2019). A review on medicinal uses of different plants of Euphorbiaceae family. *Universal Journal of Pharmaceutical Research*.

Jadhav, V., Bhagare, A., Ali, I. H., Dhayagude, A., Lokhande, D., Aher, J., [remaining authors to be verified], & Dutta, M. (2022). Role of *Moringa oleifera* on green synthesis of metal/metal oxide nanomaterials. *Journal of Nanomaterials*, **2022**, Article 2147393.

Jeyapaul, U., Kala, M. J., Bosco, A. J., Piruthiviraj, P., & Easuraja, M. (2018). An eco-friendly approach for synthesis of platinum nanoparticles using leaf extracts of *Jatropha gossypifolia* and *Jatropha glandulifera* and its antibacterial activity. *Oriental Journal of Chemistry*, **34**(2), 783.

Kanagasubbulakshmi, S., & Kadirvelu, K. (2017). Green synthesis of iron oxide nanoparticles using *Lagenaria siceraria* and evaluation of its antimicrobial activity. *Defence Life Science Journal*, **2**(4), 422–427.

Khan, S., Akhtar, N., Rehman, S. U., Shujah, S., Rha, E. S., & Jamil, M. (2020). Biosynthesized iron oxide nanoparticles (Fe_3O_4 NPs) mitigate arsenic toxicity in rice seedlings. *Toxics*, **9**(1), Article 2.

Kiwumulo, H. F., Muwonge, H., Ibingira, C., Kasozi, K. I., Namayanja, M., & Sserwanja, Q. (2022). Green synthesis and characterization of iron-oxide nanoparticles using *Moringa oleifera*: A potential protocol for use in low- and middle-income countries. *BMC Research Notes*, **15**, Article 149. https://doi.org/10.1186/s13104-022-06039-7

Kokate, C. K. (2001). *Practical pharmacognosy* (4th ed.). Vallabh Prakashan.

Laurent, S., Forge, D., Port, M., Roch, A., Robic, C., Vander Elst, L., & Muller, R. N. (2008). Magnetic iron oxide nanoparticles: Synthesis, stabilization, vectorization, physicochemical characterizations, and biological applications. *Chemical Reviews*, **108**(6), 2064–2110.

Maharjan, A., Dikshit, P. K., Gupta, A., & Kim, B. S. (2020). Catalytic activity of magnetic iron oxide nanoparticles for hydrogen peroxide decomposition: Optimization and characterization. *Journal of Chemical Technology & Biotechnology*, **95**(9), 2495–2508.

Mahire, S. P., & Patel, S. N. (2020). Extraction of phytochemicals and study of its antimicrobial and antioxidant activity of *Helicteres isora* L. *Clinical Phytoscience*, **6**, 1–6.

Nadeem, F., Fozia, F., Aslam, M., Ahmad, I., Ahmad, S., Ullah, R., [remaining authors to be verified], & Abdel-Daim, M. M. (2022). Characterization, antiplasmodial and cytotoxic activities of green synthesized iron oxide nanoparticles using *Nephrolepis exaltata* aqueous extract. *Molecules*, **27**(15), Article 4931.

Ndou, N., Rakgotho, T., Nkuna, M., Doumbia, I. Z., Mulaudzi, T., & Ajayi, R. F. (2023). Green synthesis of iron oxide (hematite) nanoparticles and their influence on *Sorghum bicolor* growth under drought stress. *Plants*, **12**(7), Article 1425.

Nikam, S. R., & Namdas, D. D. (2022). Preliminary phytochemical analysis of *Alternanthera sessilis* leaves (Linn.) R. Br. ex DC. *YMER Digital*, **21**(1), 220–225.

Osman, N. I., Sidik, N. J., Awal, A., Adam, N. A. M., & Rezali, N. I. (2016). In vitro xanthine oxidase and albumin denaturation inhibition assay of *Barringtonia racemosa* L. and total phenolic content analysis for potential anti-inflammatory use in gouty arthritis. *Journal of Intercultural Ethnopharmacology*, **5**(4), 343.

Parhizkar, J., & Habibi, M. H. (2019). Investigation and comparison of cobalt ferrite composite nanoparticles with individual iron oxide and cobalt oxide nanoparticles in azo dyes removal. *Journal of Water*

and Environmental Nanotechnology, **4**(1), 17–30.

Parveen, B., Parveen, A., Parveen, R., Ahmad, S., Ahmad, M., & Iqbal, M. (2020). Challenges and opportunities for traditional herbal medicine today, with special reference to its status in India. *Annals of Phytomedicine*, **9**(2), 97–112.

Saleem, H., Ahmad, I., Shahid, M. N., Gill, M. S. A., Nadeem, M. F., Mahmood, W., & Rashid, I. (2016). In vitro acetylcholinesterase and butyrylcholinesterase inhibitory potentials of *Jatropha gossypifolia* plant extracts. *Acta Poloniae Pharmaceutica*, **73**(2), 419–423.

Shaikh, J. R., & Patil, M. (2020). Qualitative tests for preliminary phytochemical screening: An overview. *International Journal of Chemical Studies*, **8**(2), 603–608.

Sharma, V. K., Yngard, R. A., & Lin, Y. (2009). Silver nanoparticles: Green synthesis and their antimicrobial activities. *Advances in Colloid and Interface Science*, **145**(1–2), 83–96. https://doi.org/10.1016/j.cis.2008.09.002

Song, J. Y., & Kim, B. S. (2009). Rapid biological synthesis of silver nanoparticles using plant leaf extracts. *Bioprocess and Biosystems Engineering*, **32**(1), 79–84. https://doi.org/10.1007/s00449-008-0224-6

Vishalatchi, M., Kalaiselvi, V., Yasotha, P., & Blessymol, B. (2022). Eco-friendly synthesis of ferric oxide nanoparticles—antimicrobial activity. *Journal of Environmental Nanotechnology*, **11**(3), 28–34.

Xie, M., Meng, F., Wang, P., Díaz-García, A. M., Parkhats, M., Santos-Oliveira, R., [remaining authors to be verified], & Cai, Y. (2024). Surface engineering of magnetic iron oxide nanoparticles for breast cancer diagnostics and drug delivery. *International Journal of Nanomedicine*, 8437–8461.

Yadav, R. N. S., & Agarwala, M. (2011). Phytochemical analysis of some medicinal plants. *Journal of Phytology*, **3**(12).

Yew, Y. P., Shameli, K., Miyake, M., Kuwano, N., Bt Ahmad Khairudin, N. B., Bt Mohamad, S. E., & Lee, K. X. (2016). Green synthesis of magnetite (Fe_3O_4) nanoparticles using seaweed (*Kappaphycus alvarezii*) extract. *Nanoscale Research Letters*, **11**, Article 276.

Zakariya, N. A., Majeed, S., & Jusof, W. H. W. (2022). Investigation of antioxidant and antibacterial activity of iron oxide nanoparticles (IONPs) synthesized from the aqueous extract of *Penicillium* spp. *Sensors International*, **3**, Article 100164.

Zambri, N. D. S., Taib, N. I., Abdul Latif, F., & Mohamed, Z. (2019). Utilization of neem leaf extract on biosynthesis of iron oxide nanoparticles. *Molecules*, **24**(20), Article 3803. https://doi.org/10.3390/molecules24203803

Zengin, G., Mahomoodally, M. F., Sinan, K. I., Ak, G., Etienne, O. K., Sharmeen, J. B., [remaining authors to be verified], & Ferrante, C. (2021). Chemical composition and biological properties of two *Jatropha* species: Different parts and different extraction methods. *Antioxidants*, **10**(5), Article 792.